JCM
Journals.ASM.org

Fatal Systemic Necrotizing Infections Associated with a Novel Paramyxovirus, Anaconda Paramyxovirus, in Green Anaconda Juveniles

Patrick C. Y. Woo,[a,b,c,d] Susanna K. P. Lau,[a,b,c,d] Paolo Martelli,[e] Suk-Wai Hui,[e] Candy C. Y. Lau,[b] Rachel Y. Y. Fan,[b] Joseph M. Groff,[f] Emily W. T. Tam,[b] Kwok-Hung Chan,[b] Kwok-Yung Yuen[a,b,c,d]

State Key Laboratory of Emerging Infectious Diseases,[a] Department of Microbiology,[b] Research Centre of Infection and Immunology,[c] and Carol Yu Centre for Infection,[d] The University of Hong Kong, Hong Kong; Ocean Park Corporation, Hong Kong[e]; School of Veterinary Medicine, University of California, Davis, California, USA[f]

Beginning in July 2011, 31 green anaconda (*Eunectes murinus*) juveniles from an oceanarium in Hong Kong died over a 12-month period. Necropsy revealed at least two of the following features in 23 necropsies: dermatitis, severe pan-nephritis, and/or severe systemic multiorgan necrotizing inflammation. Histopathological examination revealed severe necrotizing inflammation in various organs, most prominently the kidneys. Electron microscopic examination of primary tissues revealed intralesional accumulations of viral nucleocapsids with diameters of 10 to 14 nm, typical of paramyxoviruses. Reverse transcription (RT)-PCR results were positive for paramyxovirus (viral loads of 2.33×10^4 to 1.05×10^8 copies/mg tissue) in specimens from anaconda juveniles that died but negative in specimens from the two anaconda juveniles and anaconda mother that survived. None of the other snakes in the park was moribund, and RT-PCR results for surveillance samples collected from other snakes were negative. The virus was isolated from BHK21 cells, causing cytopathic effects with syncytial formation. The virus could also replicate in 25 of 27 cell lines of various origins, in line with its capability for infecting various organs. Electron microscopy with cell culture material revealed enveloped virus with the typical "herringbone" appearance of helical nucleocapsids in paramyxoviruses. Complete genome sequencing of five isolates confirmed that the infections originated from the same clone. Comparative genomic and phylogenetic analyses and mRNA editing experiments revealed a novel paramyxovirus in the genus *Ferlavirus*, named anaconda paramyxovirus, with a typical *Ferlavirus* genomic organization of 3′-N-U-P/V/I-M-F-HN-L-5′. Epidemiological and genomic analyses suggested that the anaconda juveniles acquired the virus perinatally from the anaconda mother rather than from other reptiles in the park, with subsequent interanaconda juvenile transmission.

Paramyxoviruses are enveloped, negative-stranded RNA viruses that are divided into two subfamilies, *Paramyxovirinae* and *Pneumovirinae*. In the past decade, a number of paramyxoviruses in the subfamily *Paramyxovirinae*, as well as their natural hosts, have been discovered. Examples include Tuhoko virus 1, 2, and 3 from fruit bats (1), Tailam virus from Sikkim rats (2), Beilong virus from brown rats and black rats (3, 4), feline morbillivirus from domestic cats (5), porcine parainfluenza virus 1 from swine (6), Menangle virus from pigs (7), Tioman virus from fruit bats (8), Cedar virus from Australian bats (9), tupaia paramyxovirus from tree shrews (10), Salem virus from horses (11), Mossman virus from rodents (12), J virus from mice (13), *Tursiops truncatus* parainfluenza virus type 1 from dolphins (14), Sunshine virus from snakes (15), and >60 new paramyxoviruses from bats and rodents (16). Traditionally, there are five genera within the subfamily *Paramyxovirinae*, namely, *Respirovirus*, *Rubulavirus*, *Morbillivirus*, *Henipavirus*, and *Avulavirus*. Recently, two new genera, i.e., *Aquaparamyxovirus*, which consists of Atlantic salmon paramyxovirus, and *Ferlavirus*, which consists of Fer-de-Lance virus (FDLV) discovered in the common lancehead snake (*Bothrops atrox*) (17, 18) (http://ictvonline.org/virusTaxonomy.asp), were proposed. In addition, there are a number of paramyxoviruses of the subfamily *Paramyxovirinae* that are still not classified into any genus; these include Beilong virus, J virus, and Tailam virus, which probably belong to the same genus (2, 13, 19), and tupaia paramyxovirus (10).

Beginning in July 2011, 31 green anaconda (*Eunectes murinus*) juveniles from Ocean Park of the Hong Kong Special Administrative Region (HKSAR) died over a 12-month period. These green anaconda juveniles were born in July 2011 from a new reptile in Ocean Park Hong Kong that had been purchased from Japan in June 2011. Since FDLV has been shown to be associated with fatalities in snakes, we hypothesized that a FDLV-like virus could be the cause of the cluster of infections. To test this hypothesis, we carried out a molecular study with samples collected from 13 of these green anaconda juveniles that died. Further viral studies and complete genomic analyses of five isolates revealed a novel paramyxovirus closely related to FDLV. In this article, we report this unprecedented cluster of fatal infections associated with a paramyxovirus in snakes and the characterization of this novel paramyxovirus, which we propose to be named anaconda paramyxovirus (AnaPV).

Received 13 June 2014 **Returned for modification** 8 July 2014
Accepted 21 July 2014
Published ahead of print 30 July 2014
Editor: E. Munson
Address correspondence to Patrick C. Y. Woo, pcywoo@hku.hk, or Kwok-Yung Yuen, kyyuen@hkucc.hku.hk.
P.C.Y.W., S.K.P.L., and P.M. contributed equally to this article.
Supplemental material for this article may be found at http://dx.doi.org/10.1128/JCM.01653-14.

doi:10.1128/JCM.01653-14

MATERIALS AND METHODS

Setting. Ocean Park Hong Kong is a financially independent, nonprofit, marine mammal park, oceanarium, animal theme park, and amusement park in Hong Kong. The park covers an area of >800,000 m^2 and is separated by a mountain into two areas, i.e., the Headland and the Lowland. The park houses >15,000 marine and terrestrial animals of >500 species. The mother of the green anaconda juveniles arrived at the park from Japan in June 2011 and was housed in the Rainforest Facility in the Headland.

Necropsies of green anaconda juveniles and sample collection. Necropsies were performed by veterinary surgeons at Ocean Park for all 31 green anaconda juveniles that died during a 12-month period (August 2011 to July 2012). Samples were collected from lungs, brain, heart, spleen, liver, kidney, gallbladder, thyroid, intestine, pancreas, skin, stomach, subcutaneous necrotic tissue, esophagus, trachea, urine, feces, and pericardial fluid. Tissue samples were fixed in 10% neutral buffered formalin for histological processing. Portions of the tissue samples from 13 green anaconda juveniles were also submerged in viral transport medium for RNA extraction and virus isolation. Formalin-fixed tissues were obtained from paraffin blocks for transmission electron microscopic (EM) examination. Tissues were deparaffinized in xylene overnight prior to rehydration through a graded ethanol series, placed in modified Karnovsky's fixative (50% strength), and postfixed with 1% osmium tetroxide. After osmification, tissues were rinsed in 0.1 M sodium cacodylate, dehydrated through a graded ethanol series, transitioned through propylene oxide, and infiltrated with and embedded in Eponate 12 epoxy formulation (Ted Pella Inc., Redding, CA). Thick toluidine blue O-stained sections were examined by light microscopy. Thin sections were mounted on 300-mesh copper grids and stained with 4% uranyl acetate in 75% ethanol, followed by poststaining with lead citrate. The grids were examined in a Zeiss 906E transmission electron microscope at 80-kV accelerating voltage (Carl Zeiss SMT, Peabody, MA).

RNA extraction. Viral RNA was extracted from the specimens using RNeasy Mini spin columns (Qiagen, Hilden, Germany) (6, 20, 21). The RNA was eluted with 50 μl of RNase-free water and was used as the template for reverse transcription (RT)-PCR.

RT-PCR of L gene of reptilian paramyxovirus and DNA sequencing. Viral RNA was extracted from the tissue samples using a QIAamp viral RNA minikit (Qiagen). Reptilian paramyxovirus detection was performed by amplifying a 178-bp fragment of the L gene of FDLV using primers LPW19205 (5′-GTATTATATGTTGCAGACCCA-3′) and LPW19206 (5′-CTGTCTGGACTGCAGCTA-3′). Reverse transcription was performed using the SuperScript III kit (Invitrogen, San Diego, CA). The PCR mixture (25 μl) contained cDNA, PCR buffer (10 mM Tris-HCl [pH 8.3], 50 mM KCl, 3 mM $MgCl_2$, and 0.01% gelatin), 200 μM each deoxynucleoside triphosphate (dNTP), and 1.0 U *Taq* polymerase (Applied Biosystems, Foster City, CA). The mixtures were amplified with 60 cycles of 94°C for 1 min, 50°C for 1 min, and 72°C for 1 min, with a final extension at 72°C for 10 min, in an automated thermal cycler (Applied Biosystems, Foster City, CA). Standard precautions were taken to avoid PCR contamination, and no false-positive results were observed for negative-control samples.

The PCR products were gel purified using the QIAquick gel extraction kit (Qiagen, Hilden, Germany). Both strands of the PCR products were sequenced twice with an ABI Prism 3700 DNA analyzer (Applied Biosystems, Foster City, CA), using the two PCR primers. The sequences of the PCR products were compared with known sequences of the L genes of paramyxoviruses in the GenBank database.

Quantitative real-time RT-PCR. All samples that were positive for AnaPV by RT-PCR were subjected to quantitative real-time RT-PCR according to our previous protocol (22). Briefly, total RNA was extracted from samples with RNeasy Mini spin columns (Qiagen, Hilden, Germany) and was reverse transcribed and amplified with AnaPV primers 5′-GCTGCCCTGAGCCTATCTGT-3′ (forward), 5′-GCTGTTGGGTTGTTCGTGAA-3′ (reverse), and 5′-FAM-CTGGTGCCTTTCTCAGCCTCTTGGTTCT-BHQ1–3′ (probe) (FAM indicates 6-carboxyfluorescein, and BHQ1 indicates black hole quencher 1) using a real-time one-step quantitative RT-PCR assay. Reaction mixtures were incubated at 50°C for 30 min and then at 95°C for 2 min and then were thermal cycled for 50 cycles of 95°C for 15 s and 55°C for 30 s. A series of 6 $\log_{10}$ dilutions, equivalent to 10^1 to 10^6 copies per reaction mixture, were prepared to generate calibration curves and were assayed in parallel with the test samples.

Complete genome sequencing. Five complete genomes of AnaPV were amplified and sequenced with an ABI Prism 3700 DNA analyzer, using the RNA extracted directly from the tissue specimens as the templates. The RNA was converted to cDNA by a combined random priming and oligo(dT) priming strategy. The cDNA was amplified with degenerate primers designed by multiple alignments of the genomes of FDLV and closely related paramyxoviruses with the complete genomes available, using strategies described in our previous publications (1, 2, 5). Additional primers were designed from the results of the first and subsequent rounds of sequencing. The 5′ ends of the viral genomes were confirmed by rapid amplification of cDNA ends (RACE) using the 5′/3′ RACE kit (Roche, Germany). Sequences were assembled and manually edited to produce final sequences of the viral genomes.

Genome analysis. The nucleotide sequences of the genomes and the deduced amino acid sequences of the open reading frames (ORFs) were compared with those of other paramyxoviruses using EMBOSS Needle (http://www.ebi.ac.uk/Tools/psa/emboss_needle). Phylogenetic tree construction was performed using the maximum likelihood method with Mega 5.0.

Analysis of P mRNA editing. To examine the number of G insertions at the P mRNA editing site, mRNA from the original specimens was extracted using the Oligotex mRNA minikit (Qiagen). First-strand cDNA synthesis was performed using the SuperScript III kit (Invitrogen) with oligo(dT) primers. The primers 5′-CCAGACAGCAAAGGTCTCAA-3′ and 5′-ACTCTCCACAGATGCAGACTT-3′ were used to amplify a 281-bp product of AnaPV covering the putative editing site. PCR was then performed with a PCR mixture (25 μl) containing cDNA, PCR buffer (10 mM Tris-HCl [pH 8.3], 50 mM KCl, 2 mM $MgCl_2$, and 0.01% gelatin), 200 μM each dNTP, and 1.0 U *Taq* polymerase (Applied Biosystems, Foster City, CA). The mixtures were amplified with 40 cycles of 94°C for 1 min, 50°C for 1 min, and 72°C for 1 min, with a final extension at 72°C for 10 min, in an automated thermal cycler (Applied Biosystems, Foster City, CA). The products were then purified and cloned using the TOPO TA cloning kit (Invitrogen, San Diego, CA). Colonies were picked randomly for sequencing analysis.

Viral cultures and EM. Viral culturing and EM were performed according to our previous publications (5, 23). Two hundred microliters of the five samples used for complete genome sequencing was subjected to viral culturing. After centrifugation, the samples were diluted 10-fold with viral transport medium and filtered. Two hundred microliters of the filtrate was inoculated into 200 μl of minimum essential medium (MEM) (Gibco, Grand Island, NY) with Polybrene. Four hundred microliters of the mixture was added to 24-well tissue culture plates with BHK21 baby hamster kidney cells by adsorption inoculation. After 1 h of adsorption, excess inoculum was discarded, the wells were washed twice with phosphate-buffered saline, and the medium was replaced with 1 ml of serum-free MEM supplemented with 0.1 μg/ml L-1-tosylamide-2-phenylethyl chloromethyl ketone (TPCK)-treated trypsin (Sigma). Cultures were incubated at 30°C with 5% CO_2 and were inspected daily, by inverted microscopy, for cytopathic effects (CPEs). After 2 to 3 weeks of incubation, subculturing in fresh cell lines was performed even if there was no CPE, and culture lysates were collected for RT-PCR for AnaPV. EM was performed with samples that were RT-PCR positive for AnaPV.

Infection and replication of AnaPV in other cell lines. Examination of the plausibility of AnaPV infecting and replicating in a variety of other cell lines was performed as described previously (24). Twenty-seven cell lines derived from different tissues or organs and host species (see Table

TABLE 1 Number of deaths associated with AnaPV infections from July 2011 to November 2012

Date	No. of deaths
July 2011	0
August 2011	3
September 2011	5
October 2011	12
November 2011	1
December 2011	3
January 2012	3
February 2012	0
March 2012	1
April 2012	0
May 2012	1
June 2012	0
July 2012	1
August 2012	0
September 2012	0
October 2012	0
November 12	0

S1 in the supplemental material) were prepared in 24-well plates and inoculated with AnaPV at a multiplicity of infection of 1 for 1 h. Nonattached virus was removed by washing the cells twice in serum-free MEM. The cells in monolayers and the cells in suspension were maintained in MEM supplemented with 0.1 μg/ml of TPCK-treated trypsin (Sigma). All infected cell lines were incubated at 30°C in 5% CO_2 for 5 days. CPEs were examined on days 1, 3, and 5 by inverted light microscopy. Total nucleic acids were extracted on days 1, 3, and 5 from culture supernatants from the 27 cell lines infected by AnaPV, using the EZ1 Virus minikit v2.0 (Qiagen, Hilden, Germany), according to the manufacturer's instructions. Quantitative real-time RT-PCR was performed as described above.

Nucleotide sequence accession numbers. The nucleotide sequences of the five genomes of AnaPV have been deposited in the GenBank sequence database under accession numbers KJ956404 to KJ956408.

RESULTS

Epidemiological data and necropsies. Thirty-three green anaconda juveniles were born on 10 July 2011 at Ocean Park. One anaconda died of trauma on 11 July 2011. Between August 2011 and July 2012, 30 additional green anaconda juveniles died (Table 1). Of the 31 green anaconda juveniles for which necropsies were performed, the carcasses of two were too autolyzed for diagnostic purposes. In the other 29 necropsies, the anacondas showed a combination of dermatitis and features suggesting infection and inflammation of various internal organs, such as nephritis, pneumonia, hepatitis, pancreatitis, and gastritis. Specifically, the affected organs were firm and swollen, with mottled pallor. The renal and hepatic capsular surfaces contained white plaques of various sizes. Cut sections revealed multiple, white, nodular, 1- to 3-mm foci of the parenchyma. The necropsies revealed that the causes of the deaths were dermatitis and subcutaneous cellulitis, severe pan-nephritis, or severe systemic necrotizing inflammation in multiple organs, including a combination of lungs, kidneys, intestine, liver, integument, spleen, thymus, pancreas, heart, and stomach, with the skin and kidneys being most severely affected. At least two of the following three features were observed in 23 necropsies: dermatitis, severe pan-nephritis, and/or severe systemic multiorgan necrotizing inflammation. No abnormalities were observed in the green anaconda mother or the two anacondas that survived. All clinical and necropsy samples were negative in bacterial and fungal cultures.

Microscopic examination results corroborated the gross findings. The most severe lesions occurred in the kidneys of all green anaconda juveniles. There was acute/subacute, severe, multifocal/diffuse, necrotizing, heterophilic inflammation of the renal parenchyma, with variable but often severe abundance of multinucleated syncytial cells. Similar lesions occurred in other organs but were often less severe and extensive than the renal lesions. EM revealed intralesional accumulations of viral nucleocapsids with diameters of 10 to 14 nm, typical of paramyxovirus, although discrete viral particles were not observed.

Identification of reptilian paramyxovirus from green anaconda juveniles. A total of 139 specimens, from 13 green anaconda juveniles that died and the two green anaconda juveniles and green anaconda mother that survived, were obtained for viral studies (Table 2). The results of RT-PCR assays for a 178-bp fragment in the L genes of paramyxoviruses were positive for specimens from the 13 green anaconda juveniles that died but negative for the specimens obtained from the two green anaconda juveniles (fecal and blood samples collected in April to July 2012) and the green anaconda mother (fecal samples collected in November 2011 to April 2012) that survived. Sequencing results showed that the sequences of all of the positive bands were identical, suggesting the presence of a paramyxovirus related to FDLV.

Viral load. A median of 5.11×10^6 copies of AnaPV RNA per mg of tissue (range, 2.33×10^4 to 1.05×10^8 copies per mg) was observed in the necropsy specimens positive for AnaPV (Table 2).

Genomic organization and coding potential of AnaPV. Complete genome sequences of five isolates of AnaPV, from two kidney samples (1110RN043 and 1201RN003), two intestine samples (1110RN047 and 1201RN001), and one necrotic tissue sample (1203RN009), from five green anaconda juveniles were determined. The genome sizes of all five isolates were 15,378 bases, and the G+C contents were 43.3%. The genome of AnaPV conforms to the rule of six, as in other paramyxovirus genomes; it contains a 55-nucleotide complementary 3′ leader and a 36-nucleotide 5′ trailer sequence.

Similar to FDLV, the genome of AnaPV contains seven genes (3′-N-U-P/V/I-M-F-HN-L-5′) (Fig. 1). Pairwise alignment of the predicted gene products among AnaPV and other paramyxoviruses showed the highest amino acid identities with FDLV, with the N, U, P/V/I(P), P/V/I(V), P/V/I(I), M, F, HN, and L genes of AnaPV having 97.2%, 75.4%, 87.2%, 83.7%, 79.4%, 97.4%, 95.6%, 93.3 to 93.5%, and 96.8% amino acid identities, respectively, to those of FDLV (see Table S2 in the supplemental material). The sequences of the five genomes were identical except at three positions, confirming the presence of the same strain of AnaPV in these five anacondas. Using isolate 1110RN043 as the reference, isolate 1201RN001 contains a synonymous mutation (C→T) at base 2996 and a nonsynonymous mutation (A→G; Ile→Val) at base 8078 and isolate 1203RN009 contains a synonymous mutation (A→G) at base 656 (Fig. 1). The lengths and characteristics of the major structural genes and intergenic regions are summarized in Table S3 in the supplemental material.

As in FDLV, a unique gene, U, is present between the N and P/V/I genes in the genome of AnaPV. This is the gene in the AnaPV genome that possesses the lowest amino acid identity to that of FDLV. However, it possesses higher amino acid identities to those of some other reptilian paramyxoviruses. Furthermore,

TABLE 2 RT-PCR and quantitative real-time RT-PCR results for samples collected from 13 dead green anaconda juveniles that underwent necropsy

Anaconda juvenile no.	Sample collection date (day/mo/yr)	Sample identification[a]	AnaPV RT-PCR result	Viral load (RNA copies per mg tissue or ml fecal sample)
001	19/10/2011	1110RN041/stomach mucus	−	
	19/10/2011	1110RN041/lung/liver/kidney/spleen	+	1.34×10^6
002	19/10/2011	1110RN043/liver	−	
	19/10/2011	1110RN043/kidney	+	4.48×10^4
	19/10/2011	1110RN043/spleen	−	
003	31/10/2011	1110RN047/kidney	−	
	31/10/2011	1110RN047/intestine	+	1.74×10^7
	31/10/2011	1110RN047/brain	−	
	31/10/2011	1110RN047/gallbladder	−	
	31/10/2011	1110RN047/stomach	−	
	31/10/2011	1110RN047/esophagus	−	
	31/10/2011	1110RN047/liver	−	
	31/10/2011	1110RN047/lungs	−	
	31/10/2011	1110RN047/heart	−	
	31/10/2011	1110RN047/tracheas	−	
	31/10/2011	1110RN047/brain	−	
	31/10/2011	1110RN047/lung/liver/kidney/spleen	−	
013	8/1/2012	1201RN001/heart	−	
	8/1/2012	1201RN001/lung	+	2.30×10^6
	8/1/2012	1201RN001/liver	+	3.62×10^5
	8/1/2012	1201RN001/kidney	−	
	8/1/2012	1201RN001/brain	−	
	8/1/2012	1201RN001/stomach	+	2.33×10^4
	8/1/2012	1201RN001/intestine	+	7.85×10^7
	8/1/2012	1201RN001/skin	+	1.07×10^7
035	27/12/2011	1112RN058/heart	−	
	27/12/2011	1112RN058/lung	+	1.26×10^5
	27/12/2011	1112RN058/liver	+	1.29×10^6
	27/12/2011	1112RN058/spleen	−	
	27/12/2011	1112RN058/pancreas	+	3.03×10^5
	27/12/2011	1112RN058/kidney	+	2.34×10^7
264	21/1/2012	1201RN003/spleen	−	
	21/1/2012	1201RN003/heart	+	1.06×10^6
	21/1/2012	1201RN003/brain	−	
	21/1/2012	1201RN003/small intestine and feces	+	1.05×10^8
	21/1/2012	1201RN003/kidney	+	4.23×10^7
	21/1/2012	1201RN003/lung	+	5.57×10^6
	21/1/2012	1201RN003/liver	+	1.88×10^7
	21/1/2012	1201RN003/granuloma on stomach	+	7.40×10^5
535	7/12/2011	1112RN052/skin	+	5.52×10^6
	7/12/2011	1112RN052/kidney	+	5.65×10^6
	7/12/2011	1112RN052/liver	+	9.92×10^4
	7/12/2011	1112RN052/thyroid	+	3.85×10^7
	7/12/2011	1112RN052/heart	−	
	7/12/2011	1112RN052/lung	+	5.53×10^7
	7/12/2011	1112RN052/spleen	−	
	7/12/2011	1112RN052/gastric	+	1.03×10^7
	7/12/2011	1112RN052/fecal swab	−	
	7/12/2011	1112RN052/intestine	+	3.07×10^7
	7/12/2011	1112RN052/brain	−	
554	15/12/2011	1112RN053/heart	−	
	15/12/2011	1112RN053/kidney	+	2.37×10^7
	15/12/2011	1112RN053/intestine	+	3.37×10^7
	15/12/2011	1112RN053/liver	+	8.23×10^5

(Continued on following page)

TABLE 2 (Continued)

Anaconda juvenile no.	Sample collection date (day/mo/yr)	Sample identification[a]	AnaPV RT-PCR result	Viral load (RNA copies per mg tissue or ml fecal sample)
	15/12/2011	1112RN053/lung	+	1.24×10^7
	15/12/2011	1112RN053/skin	−	
	15/12/2011	1112RN053/subcutaneous lesion	−	
	15/12/2011	1112RN053/stomach	−	
	15/12/2011	1112RN053/trachea	−	
573	5/5/2012	1205RN015/colon	+	4.70×10^6
	5/5/2012	1205RN015/pancreas	+	2.19×10^6
	5/5/2012	1205RN015/kidney	+	2.57×10^6
	5/5/2012	1205RN015/skin	−	
	5/5/2012	1205RN015/lungs	+	7.84×10^6
	5/5/2012	1205RN015/heart	−	
	5/5/2012	1205RN015/liver	−	
	5/5/2012	1205RN015/spleen	−	
	5/5/2012	1205RN015/duodenum	+	4.42×10^7
620	22/11/2011	1111RN049/fecal swab	+	1.90×10^8
	22/11/2011	1111RN049/intestine	+	4.19×10^5
	22/11/2011	1111RN049/kidney	+	3.54×10^7
	22/11/2011	1111RN049/liver	−	
	22/11/2011	1111RN049/lung	−	
771	10/1/2012	1201RN002/GI tract	+	2.45×10^5
	10/1/2012	1201RN002/liver	+	7.40×10^4
	10/1/2012	1201RN002/lung	+	2.13×10^6
	10/1/2012	1201RN002/heart	−	
	10/1/2012	1201RN002/kidney	+	3.92×10^6
	10/1/2012	1201RN002/spleen	+	1.04×10^6
	10/1/2012	1201RN002/trachea	−	
834	13/7/2012	1207RN022/brain	−	
	13/7/2012	1207RN022/heart	−	
	13/7/2012	1207RN022/lung	+	1.25×10^7
	13/7/2012	1207RN022/stomach	−	
	13/7/2012	1207RN022/spleen	−	
	13/7/2012	1207RN022/liver	−	
	13/7/2012	1207RN022/pancreas	−	
	13/7/2012	1207RN022/left kidney	−	
	13/7/2012	1207RN022/right kidney	+	8.46×10^6
849	16/3/2012	1203RN009/brain	−	
	16/3/2012	1203RN009/fecal sample	−	
	16/3/2012	1203RN009/kidney	−	
	16/3/2012	1203RN009/liver	−	
	16/3/2012	1203RN009/lung	−	
	16/3/2012	1203RN009/pericardial fluid	−	
	16/3/2012	1203RN009/spleen	−	
	16/3/2012	1203RN009/stomach	−	
	16/3/2012	1203RN009/subcutaneous necrotic tissue	+	1.23×10^6

[a] GI, gastrointestinal.

the putative initiation site of U in AnaPV is different from that in FDLV, supporting this gene's relatively distant relationship to that of FDLV (see Fig. S1A in the supplemental material).

As in FDLV, the P/V/I gene of AnaPV contains one initiation codon. Similar to those of most members of *Paramyxovirinae*, the P/V/I gene of AnaPV contains a UC-rich editing site that allows the addition of nontemplated G residues to mRNA products during P/V/I gene transcription, resulting in the production of different proteins with a common N-terminal region. In the five isolates of AnaPV sequenced, this common N-terminal region consists of 158 amino acids. In FDLV, a short SB ORF, encoding a putative 53-amino acid protein, is present upstream of the editing site (25). However, this ORF is prematurely terminated in AnaPV, encoding a putative protein of only 26 amino acids, with a loss of >50% of the basic amino acids (see Fig. S1B in the supplemental material).

Similar to FDLV, the F protein of AnaPV has a multibasic protein cleavage site with the consensus sequence R-X-R/K-R, as

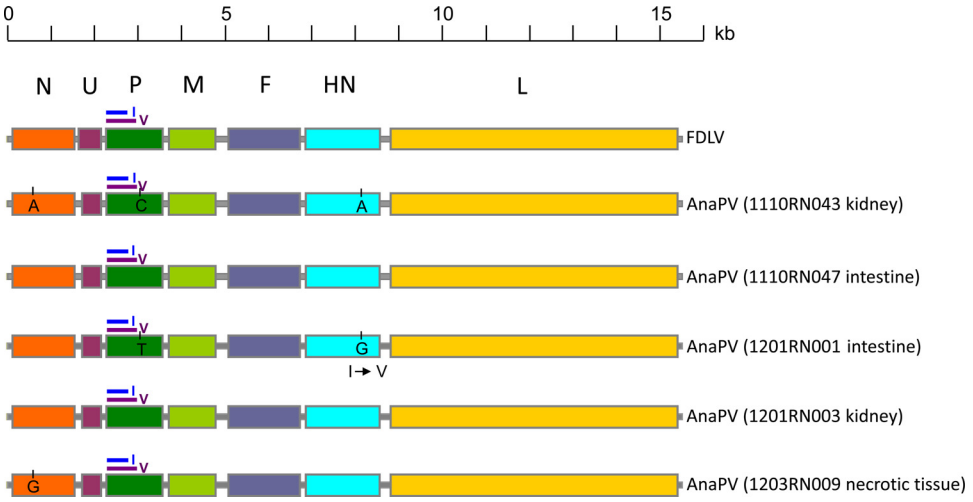

FIG 1 Genomic organization of AnaPV and FDLV. The genes are shown as boxes that are drawn to scale. For the P gene, the purple line above the green box represents the region V coding DNA sequence (CDS) and the blue line represents the region I CDS. Single-nucleotide polymorphisms of the five AnaPV genomes (1201RN001, 1110RN043, 1110RN047, 1201RN003, and 1203RN009) sequenced are shown.

in other paramyxoviruses (25). A cellular trypsin-like protease cleaves the F protein into F_1 and F_2 before cell fusion occurs, which facilitates the isolation of these viruses in cell lines. Two heptad repeat sequences, similar to those in the F proteins of other paramyxoviruses, were identified in the F_1 peptide of AnaPV. The F protein of AnaPV contains two potential *N*-glycosylation sites in the F_1 peptide but no potential *N*-glycosylation sites in the F_2 peptide, in contrast to the F protein of FDLV, which contains two potential *N*-glycosylation sites in the F_1 peptide and one potential *N*-glycosylation site in the F_2 peptide.

mRNA editing of AnaPV. To determine the exact location of the P gene editing site and the number and frequency of G-residue insertions, a small cDNA fragment including the UC-rich region was amplified, cloned, and sequenced using mRNA extracted from AnaPV-infected BHK21 cells. Among 37 independent clones sequenced, 31 contained the sequence GTAAGGGGGG (without a G insertion, encoding V protein), two contained the sequence GTAAGGGGGGG (one G inserted, encoding I protein), and four contained the sequence GTAAGGGGGGGG (two Gs inserted, encoding P protein). In most other paramyxoviruses except rubulaviruses, the sequence A_nG_n is conserved in the mRNA editing sites. In FDLV, however, this sequence is $ATAAG_n$; in AnaPV, this sequence is $GTAAG_n$.

Phylogenetic analyses. Phylogenetic trees constructed using the predicted amino acid sequences of the N, U, P, V, M, F, HN, and L genes of AnaPV and other members of *Paramyxoviridae* are shown in Fig. 2. In all eight trees, AnaPV was clustered with FDLV and other reptilian paramyxoviruses, with high bootstrap supports, forming a distinct group in *Paramyxoviridae* (Fig. 2). Notably, in the phylogenetic tree constructed using the U gene, AnaPV was most closely related to some reptilian paramyxoviruses other than FDLV, indicating that there could be more closely related reptilian paramyxoviruses but without complete genome sequences available.

Viral cultures and EM. At the third passage, BHK21 cells inoculated with a kidney sample (1110RN043) positive for AnaPV showed CPEs at day 3, with syncytial formation (Fig. 3A). RT-PCR for AnaPV using the culture supernatants and cell lysates showed positive results for BHK21 cells inoculated with the kidney sample (1110RN043). EM showed an enveloped virus with the typical "herringbone" appearance of the helical N in paramyxoviruses (Fig. 3B). Virions were highly variable in size, ranging approximately from 125 to 507 nm in diameter.

Infection and replication of AnaPV in other cell lines. Real-time quantitative RT-PCR showed significant replication of AnaPV in 25 of the 27 cell lines (see Table S1 in the supplemental material). Minimal replication was observed in the HEK and C6/36 cell lines. Among the 25 cell lines in which AnaPV showed significant replication, CPEs were also observed in RK13 and Vero cells (see Fig. S2 in the supplemental material).

DISCUSSION

We have documented a cluster of fatal infections in green anaconda juveniles associated with AnaPV, a novel paramyxovirus of the genus *Ferlavirus* in subfamily *Paramyxovirinae*. The cluster of infections was associated with a >90% mortality rate among the 33 anaconda juveniles that were progeny of the female parent that the facility purchased from Japan. All anaconda juveniles that died presented with dermatitis and subcutaneous cellulitis, severe pannephritis, or necrotizing inflammation of multiple organs, with the skin and kidneys being most severely affected. The widespread pathological findings in skin, subcutaneous tissue, and multiple internal organs were in line with the observation of high viral loads, with a median of 5.11×10^6 copies of AnaPV RNA per mg of tissue, in skin, kidney, liver, thyroid, lung, heart, pancreas, and gastrointestinal specimens obtained from the dead green anaconda juveniles (Table 2), and the *in vitro* characteristic of the virus to replicate in a large variety of cell lines from various organs and tissues (see Table S1 in the supplemental material). This pathogenic characteristic of AnaPV is similar to that observed for FDLV, which was originally discovered in a common lancehead snake during a disease outbreak in a snake farm in Zurich, Switzerland, in 1972, as well as other paramyxovirus-like agents isolated from a variety of reptile species causing epizootics with high mortality rates in snakes and other reptiles (26–30). Notably, the internal organs that showed the most serious pathologies in the

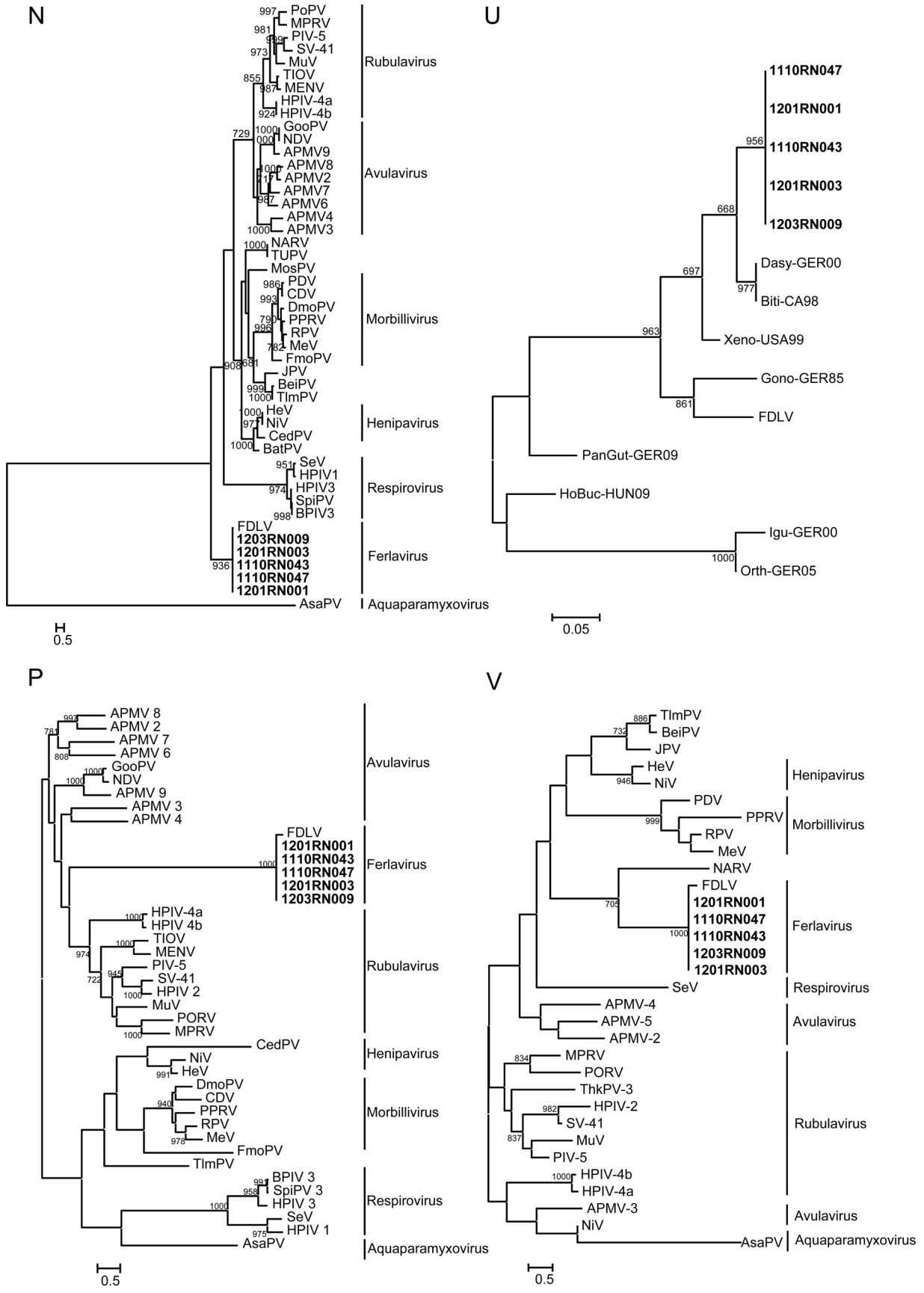
N
PoPV
MPRV
PIV-5
SV-41
MuV
TIOV
MENV
HPIV-4a
HPIV-4b
GooPV
NDV
APMV9
APMV8
APMV2
APMV7
APMV6
APMV4
APMV3
NARV
TUPV
MosPV
PDV
CDV
DmoPV
PPRV
RPV
MeV
FmoPV
JPV
BeiPV
TlmPV
HeV
NiV
CedPV
BatPV
SeV
HPIV1
HPIV3
SpiPV
BPIV3
FDLV
1203RN009
1201RN003
1110RN043
1110RN047
1201RN001
AsaPV
Rubulavirus
Avulavirus
Morbillivirus
Henipavirus
Respirovirus
Ferlavirus
Aquaparamyxovirus
0.5
U
1110RN047
1201RN001
1110RN043
1201RN003
1203RN009
Dasy-GER00
Biti-CA98
Xeno-USA99
Gono-GER85
FDLV
PanGut-GER09
HoBuc-HUN09
Igu-GER00
Orth-GER05
0.05
P
APMV 8
APMV 2
APMV 7
APMV 6
GooPV
NDV
APMV 9
APMV 3
APMV 4
FDLV
1201RN001
1110RN043
1110RN047
1201RN003
1203RN009
HPIV-4a
HPIV 4b
TIOV
MENV
PIV-5
SV-41
HPIV 2
MuV
PORV
MPRV
CedPV
NiV
HeV
DmoPV
CDV
PPRV
RPV
MeV
FmoPV
TlmPV
BPIV 3
SpiPV 3
HPIV 3
SeV
HPIV 1
AsaPV
Avulavirus
Ferlavirus
Rubulavirus
Henipavirus
Morbillivirus
Respirovirus
Aquaparamyxovirus
0.5
V
TlmPV
BeiPV
JPV
HeV
NiV
PDV
PPRV
RPV
MeV
NARV
FDLV
1201RN001
1110RN047
1110RN043
1203RN009
1201RN003
SeV
APMV-4
APMV-5
APMV-2
MPRV
PORV
ThkPV-3
HPIV-2
SV-41
MuV
PIV-5
HPIV-4b
HPIV-4a
APMV-3
NiV
AsaPV
Henipavirus
Morbillivirus
Ferlavirus
Respirovirus
Avulavirus
Rubulavirus
Avulavirus
Aquaparamyxovirus
0.5

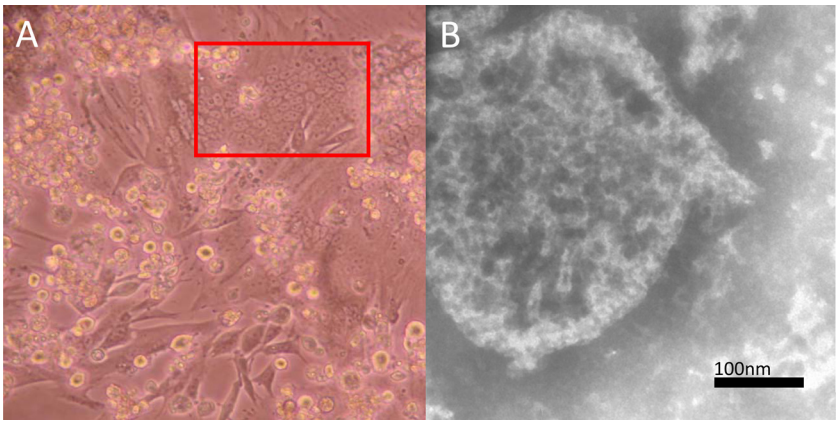

FIG 3 (A) CPEs of AnaPV on BHK21 cells. Red square, formation of syncytia. (B) EM examination of infected BHK21 cell culture supernatant, showing enveloped virus with a burst envelope and typical herringbone appearance of helical N in paramyxoviruses.

anaconda juveniles infected by AnaPV were the kidneys, whereas the organs that were most severely affected by FDLV were the lungs (18, 31, 32). It is also interesting to note that, in infections with Sunshine virus (another paramyxovirus of *Ferlavirus*) in jungle carpet pythons (*Morelia spilota cheynei*), most pythons died of neurorespiratory diseases, although the virus can be isolated from multiple organs, including lungs, liver, kidneys, and brain (28). Isolation and EM examination revealed that the size and morphology of AnaPV are typical of those of other paramyxoviruses. When the RNA extracted from the specimens from the 13 dead green anaconda juveniles were amplified and sequenced, all positive 178-bp bands showed identical sequences. Moreover, when five of the genomes, representing five different AnaPV isolates from different time points during the infection cluster, were completely sequenced, mutations were observed at only three positions in the genomes, in the N, P, and HN genes. Only one of the three mutations (the mutation in the HN gene) was a nonsynonymous mutation. These findings indicated that the AnaPV isolates were of clonal origin. We speculate that the anaconda juveniles acquired the virus from the anaconda mother perinatally, instead of from other reptiles in the park with subsequent interanaconda transmission, as there was only one peak in the early postnatal period in the epizootic curve (Table 1) and complete genome sequencing did not show any progressive mutational changes, as is the case with multiple steps of interanimal transmission (Fig. 1). Moreover, none of the other snakes in the park was moribund and RT-PCR results for the surveillance samples collected from the other snakes were all negative (data not shown). Unfortunately, no clinical samples from the anaconda mother were obtained during the perinatal period, as she did not have any abnormal clinical features at that time.

Genomic and phylogenetic analysis showed that AnaPV is most closely related to FDLV among all paramyxoviruses for which complete genome sequences are available. The genomic organization of AnaPV is identical to that of FDLV. The genomes of both AnaPV and FDLV contain seven genes (3′-N-U-P/V/I-M-F-HN-L-5′) (Fig. 1). The P/V/I genes of AnaPV and FDLV both contain one initiation codon. The U gene, located between the N and P/V/I genes in the genomes, is unique to AnaPV and FDLV and is not observed in paramyxoviruses of any other genera. Moreover, the U protein is not homologous to any known proteins. Phylogenetic analyses using N, P, V, M, F, HN, and L all showed that AnaPV is clustered with FDLV, with high bootstrap supports (Fig. 2), with the putative proteins encoded by their N,

FIG 2 Phylogenetic analyses of N, U, P, V, M, F, HN, and L amino acid sequences of AnaPV. The trees were constructed by the maximum likelihood method with bootstrap values calculated from 1,000 trees and rooted on the midpoint. Scale bars, branch lengths that correspond to 0.05 to 0.5 substitutions per site, as indicated. Five isolates from AnaPV were named 1201RN001, 1110RN043, 1110RN047, 1201RN003, and 1203RN009 (shown in bold type). DmoPV, dolphin morbillivirus (GenBank accession number NC_005283.1); PPRV, peste-des-petits ruminants virus (NC_006383); MeV, measles virus (NC_001498); CDV, canine distemper virus (NC_001921); MosPV, Mossman virus (NC_005339); ThkPV2, Tuhoko virus 2 (GU128081); JPV, J virus (NC_007454); BeiPV, Beilong virus (NC_007803); NiV, Nipah virus (NC_002728); HeV, Hendra virus (NC_001906); FDLV, Fer-de-Lance virus (NC_005084); SeV, Sendai virus (NC_001552); HPIV-1, human parainfluenza virus 1 (NC_003461); CedPV, Cedar virus (JQ001776.1); SaPV, Salem virus (JQ697837.1); PDV, phocine distemper virus (Y09630.1); FmoPV, feline morbillivirus (JQ411015.1); RPV, rinderpest virus (NC_006296.2); TUPV, tupaia paramyxovirus (NC_002199.1); TlmPV, Tailam virus (JN689227); MENV, Menangle virus (NC_007620.1); HPIV-2, human parainfluenza virus 2 (NC_003443.1); PoRV, porcine rubulavirus (NC_009640.1); NDV, Newcastle disease virus (NC_002617.1); HPIV-4a, human parainfluenza virus 4a (AB543336.1); HPIV-4b, human parainfluenza virus 4b (JQ241176.1); MuV, mumps virus (NC_002200.1); HPIV-3, human parainfluenza virus 3 (NC_001796.2); BPIV-3, bovine parainfluenza virus 3 (NC_002161.1); MPRV, Mapuera virus (NC_009489.1); PIV-5, parainfluenza virus 5 (NC_006430.1); SV-41, simian virus 41 (NC_006428.1); TIOV, Tioman virus (NC_004074.1); GooPV, goose paramyxovirus SF02 (NC_005036.1); APMV-9, avian paramyxovirus 9 strain duck/New York/22/1978 (EU910942.1); APMV-8, avian paramyxovirus 8 strain pintail/Wakuya/20/78 (FJ215864.1); APMV-7, avian paramyxovirus 7 strain APMV-7/dove/Tennessee/4/75 (FJ231524); APMV-6, avian paramyxovirus 6 (NC_003043.1); APMV-5, avian paramyxovirus 5 strain budgerigar/Kunitachi/74 (GU206351); APMV-4, avian paramyxovirus 4 isolate APMV-4/Egyptian goose/South Africa/N1468/2010 (JX133079.1); APMV-3, avian paramyxovirus 3 strain APMV3/PKT/Netherland/449/75 (EU403085); APMV-2, avian paramyxovirus 2 isolate NK (HQ896024); NARV, Nariva virus (NC_017937.1); BatPV, bat paramyxovirus Eid_hel/GH-M74a/GHA/2009 (AFH96006.1); SpiPV, swine parainfluenza 3 (EU439429.2); AsaPV, Atlantic salmon paramyxovirus strain ASPV-Ro (EF646380.1); Dasy-GER00, snake paramyxovirus (ACT63842.1); Biti-CA98, reptilian paramyxovirus (AAS45836.1); Xeno-USA99, lizard paramyxovirus (ACT63860.1); Gono-GER85, reptilian paramyxovirus (AAS45835.1); PanGut-GER09, snake paramyxovirus (ADT91317.1); HoBuc-HUN09, snake paramyxovirus (AFQ32570.1); Igu-GER00, lizard paramyxovirus (ACT63854.1); Orth-GER05, snake paramyxovirus (ACT63852.1).

M, F, HN, and L genes showing >90% amino acid identities with each other (see Table S2 in the supplemental material).

Although AnaPV showed high levels of similarity with FDLV, to include them within the same genus, AnaPV should be a novel paramyxovirus because its genome possessed characteristics distinct from those of FDLV. The SB ORF of AnaPV, upstream of the UC-rich editing site in FDLV, is prematurely terminated. In AnaPV, the P gene editing site sequence is $GTAAG_n$; in FDLV, the P gene editing site sequence is $ATAAG_n$. The F_2 peptide of AnaPV does not possess a potential *N*-glycosylation site. This is different from FDLV, which possesses one potential *N*-glycosylation site. The putative proteins encoded by the U, P, V, and I genes of AnaPV possess only 75.6% to 87.2% amino acid identities with respect to those of FDLV. The putative initiation site for the U gene in AnaPV is also different from that in FDLV (see Fig. S1A in the supplemental material). Importantly, for the phylogenetic trees constructed using the U protein and the partial protein from other available reptilian paramyxoviruses, a number of sequences were observed for AnaPV and FDLV (Fig. 2; also see Fig. S3 in the supplemental material). These various sequences showed that AnaPV and FDLV are two distinct members of the genus *Ferlavirus*, infecting different hosts. The present study highlights the importance of complete genome sequencing for characterization of novel viruses. Discovery and complete genome sequencing of other reptilian paramyxoviruses and comparative genomic and phylogenetic analyses will yield a better phylogenetic map of this genus of paramyxoviruses, which has endangered the reptilian populations in snake farms and zoological collections.

ACKNOWLEDGMENTS

We thank Wing-Man Ko, Secretary for Food and Health, and Constance Chan, Director of the Department of Health, HKSAR, Peoples' Republic of China, for their continuous support. We also thank the Veterinary Department and Clinical Laboratory of the Ocean Park Corp. for specimen collection and Robert W. Nordhausen for assistance with electron microscopy.

This work was partly supported by a Research Grants Council grant from the University Grants Committee, the Consultancy Service for Enhancing Laboratory Surveillance of Emerging Infectious Disease for the HKSAR Department of Health, the HKSAR Health and Medical Research Fund, and the Strategic Research Theme Fund of the University of Hong Kong.

REFERENCES

1. **Lau SK, Woo PC, Wong BH, Wong AY, Tsoi HW, Wang M, Lee P, Xu H, Poon RW, Guo R, Li KS, Chan KH, Zheng BJ, Yuen KY.** 2010. Identification and complete genome analysis of three novel paramyxoviruses, Tuhoko virus 1, 2 and 3, in fruit bats from China. Virology **404:**106–116. http://dx.doi.org/10.1016/j.virol.2010.03.049.
2. **Woo PC, Lau SK, Wong BH, Wong AY, Poon RW, Yuen KY.** 2011. Complete genome sequence of a novel paramyxovirus, Tailam virus, discovered in Sikkim rats. J. Virol. **85:**13473–13474. http://dx.doi.org/10.1128/JVI.06356-11.
3. **Woo PC, Lau SK, Wong BH, Wu Y, Lam CS, Yuen KY.** 2012. Novel variant of Beilong paramyxovirus in rats, China. Emerg. Infect. Dis. **18:**1022–1024. http://dx.doi.org/10.3201/eid1806.111901.
4. **Li Z, Yu M, Zhang H, Magoffin DE, Jack PJ, Hyatt A, Wang HY, Wang LF.** 2006. Beilong virus, a novel paramyxovirus with the largest genome of non-segmented negative-stranded RNA viruses. Virology **346:**219–228. http://dx.doi.org/10.1016/j.virol.2005.10.039.
5. **Woo PC, Lau SK, Wong BH, Fan RY, Wong AY, Zhang AJ, Wu Y, Choi GK, Li KS, Hui J, Wang M, Zheng BJ, Chan KH, Yuen KY.** 2012. Feline morbillivirus, a previously undescribed paramyxovirus associated with tubulointerstitial nephritis in domestic cats. Proc. Natl. Acad. Sci. U. S. A. **109:**5435–5440. http://dx.doi.org/10.1073/pnas.1119972109.
6. **Lau SK, Woo PC, Wu Y, Wong AY, Wong BH, Lau CC, Fan RY, Cai JP, Tsoi HW, Chan KH, Yuen KY.** 2013. Identification and characterization of a novel paramyxovirus, porcine parainfluenza virus 1, from deceased pigs. J. Gen. Virol. **94:**2184–2190. http://dx.doi.org/10.1099/vir.0.052985-0.
7. **Bowden TR, Westenberg M, Wang LF, Eaton BT, Boyle DB.** 2001. Molecular characterization of Menangle virus, a novel paramyxovirus which infects pigs, fruit bats, and humans. Virology **283:**358–373. http://dx.doi.org/10.1006/viro.2001.0893.
8. **Chua KB, Wang LF, Lam SK, Crameri G, Yu M, Wise T, Boyle D, Hyatt AD, Eaton BT.** 2001. Tioman virus, a novel paramyxovirus isolated from fruit bats in Malaysia. Virology **283:**215–229. http://dx.doi.org/10.1006/viro.2000.0882.
9. **Marsh GA, de Jong C, Barr JA, Tachedjian M, Smith C, Middleton D, Yu M, Todd S, Foord AJ, Haring V, Payne J, Robinson R, Broz I, Crameri G, Field HE, Wang LF.** 2012. Cedar virus: a novel henipavirus isolated from Australian bats. PLoS Pathog. **8:**e1002836. http://dx.doi.org/10.1371/journal.ppat.1002836.
10. **Tidona CA, Kurz HW, Gelderblom HR, Darai G.** 1999. Isolation and molecular characterization of a novel cytopathogenic paramyxovirus from tree shrews. Virology **258:**425–434. http://dx.doi.org/10.1006/viro.1999.9693.
11. **Renshaw RW, Glaser AL, Van Campen H, Weiland F, Dubovi EJ.** 2000. Identification and phylogenetic comparison of Salem virus, a novel paramyxovirus of horses. Virology **270:**417–429. http://dx.doi.org/10.1006/viro.2000.0305.
12. **Miller PJ, Boyle DB, Eaton BT, Wang LF.** 2003. Full-length genome sequence of Mossman virus, a novel paramyxovirus isolated from rodents in Australia. Virology **317:**330–344. http://dx.doi.org/10.1016/j.virol.2003.08.013.
13. **Jack PJ, Boyle DB, Eaton BT, Wang LF.** 2005. The complete genome sequence of J virus reveals a unique genome structure in the family *Paramyxoviridae*. J. Virol. **79:**10690–10700. http://dx.doi.org/10.1128/JVI.79.16.10690-10700.2005.
14. **Nollens HH, Wellehan JF, Saliki JT, Caseltine SL, Jensen ED, Van Bonn W, Venn-Watson S.** 2008. Characterization of a parainfluenza virus isolated from a bottlenose dolphin (*Tursiops truncatus*). Vet. Microbiol. **128:**231–242. http://dx.doi.org/10.1016/j.vetmic.2007.10.005.
15. **Hyndman TH, Marschang RE, Wellehan JF, Jr, Nicholls PK.** 2012. Isolation and molecular identification of Sunshine virus, a novel paramyxovirus found in Australian snakes. Infect. Genet. Evol. **12:**1436–1446. http://dx.doi.org/10.1016/j.meegid.2012.04.022.
16. **Drexler JF, Corman VM, Muller MA, Maganga GD, Vallo P, Binger T, Gloza-Rausch F, Rasche A, Yordanov S, Seebens A, Oppong S, Adu Sarkodie Y, Pongombo C, Lukashev AN, Schmidt-Chanasit J, Stocker A, Carneiro AJ, Erbar S, Maisner A, Fronhoffs F, Buettner R, Kalko EK, Kruppa T, Franke CR, Kallies R, Yandoko ER, Herrler G, Reusken C, Hassanin A, Kruger DH, Matthee S, Ulrich RG, Leroy EM, Drosten C.** 2012. Bats host major mammalian paramyxoviruses. Nat. Commun. **3:**796. http://dx.doi.org/10.1038/ncomms1796.
17. **Falk K, Batts WN, Kvellestad A, Kurath G, Wiik-Nielsen J, Winton JR.** 2008. Molecular characterisation of Atlantic salmon paramyxovirus (ASPV): a novel paramyxovirus associated with proliferative gill inflammation. Virus Res. **133:**218–227. http://dx.doi.org/10.1016/j.virusres.2008.01.006.
18. **Clark HF, Lief FS, Lunger PD, Waters D, Leloup P, Foelsch DW, Wyler RW.** 1979. Fer de Lance virus (FDLV): a probable paramyxovirus isolated from a reptile. J. Gen. Virol. **44:**405–418. http://dx.doi.org/10.1099/0022-1317-44-2-405.
19. **Magoffin DE, Mackenzie JS, Wang LF.** 2007. Genetic analysis of J-virus and Beilong virus using minireplicons. Virology **364:**103–111. http://dx.doi.org/10.1016/j.virol.2007.01.045.
20. **Lau SK, Li KS, Chau KY, So LY, Lee RA, Lau YL, Chan KH, Lim WW, Woo PC, Yuen KY.** 2009. Clinical and molecular epidemiology of human parainfluenza virus 4 infections in Hong Kong: subtype 4B as common as subtype 4A. J. Clin. Microbiol. **47:**1549–1552. http://dx.doi.org/10.1128/JCM.00047-09.
21. **Lau SK, To WK, Tse PW, Chan AK, Woo PC, Tsoi HW, Leung AF, Li KS, Chan PK, Lim WW, Yung RW, Chan KH, Yuen KY.** 2005. Human parainfluenza virus 4 outbreak and the role of diagnostic tests. J. Clin. Microbiol. **43:**4515–4521. http://dx.doi.org/10.1128/JCM.43.9.4515-4521.2005.
22. **Lau SK, Lau CC, Chan KH, Li CP, Chen H, Jin DY, Chan JF, Woo PC, Yuen KY.** 2013. Delayed induction of proinflammatory cytokines and suppression of innate antiviral response by the novel Middle East respiratory syndrome coronavirus: implications for pathogenesis and treatment. J. Gen. Virol. **94:**2679–2690. http://dx.doi.org/10.1099/vir.0.055533-0.

23. **Lau SK, Woo PC, Yip CC, Fan RY, Huang Y, Wang M, Guo R, Lam CS, Tsang AK, Lai KK, Chan KH, Che XY, Zheng BJ, Yuen KY.** 2012. Isolation and characterization of a novel Betacoronavirus subgroup A coronavirus, rabbit coronavirus HKU14, from domestic rabbits. J. Virol. **86:**5481–5496. http://dx.doi.org/10.1128/JVI.06927-11.
24. **Chan JF, Chan KH, Choi GK, To KK, Tse H, Cai JP, Yeung ML, Cheng VC, Chen H, Che XY, Lau SK, Woo PC, Yuen KY.** 2013. Differential cell line susceptibility to the emerging novel human betacoronavirus 2c EMC/2012: implications for disease pathogenesis and clinical manifestation. J. Infect. Dis. **207:**1743–1752. http://dx.doi.org/10.1093/infdis/jit123.
25. **Kurath G, Batts WN, Ahne W, Winton JR.** 2004. Complete genome sequence of Fer-de-Lance virus reveals a novel gene in reptilian paramyxoviruses. J. Virol. **78:**2045–2056. http://dx.doi.org/10.1128/JVI.78.4.2045-2056.2004.
26. **Fölsch DW, Leloup P.** 1976. Fatal endemic infection in a serpentarium: diagnosis, treatment and preventive measures. Tierarztl. Prax. **4:**527–536. (In German.)
27. **Papp T, Gal J, Abbas MD, Marschang RE, Farkas SL.** 2013. A novel type of paramyxovirus found in Hungary in a masked water snake (*Homalopsis buccata*) with pneumonia supports the suggested new taxonomy within the Ferlavirus genus. Vet. Microbiol. **162:**195–200. http://dx.doi.org/10.1016/j.vetmic.2012.08.010.
28. **Hyndman TH, Shilton CM, Doneley RJ, Nicholls PK.** 2012. Sunshine virus in Australian pythons. Vet. Microbiol. **161:**77–87. http://dx.doi.org/10.1016/j.vetmic.2012.07.030.
29. **Kolesnikovas CK, Grego KF, Rameh de Albuquerque LC, Jacobson ER, Monezi TA, Mehnert DU, Catao-Dias JL.** 2006. Ophidian paramyxovirus in Brazilian vipers (*Bothrops alternatus*). Vet. Rec. **159:**390–392. http://dx.doi.org/10.1136/vr.159.12.390.
30. **Jacobson ER, Gaskin JM, Wells S, Bowler K, Schumacher J.** 1992. Epizootic of ophidian paramyxovirus in a zoological collection: pathological, microbiological, and serological findings. J. Zoo Wildl. Med. **23:**318–327.
31. **Homer BL, Sundberg JP, Gaskin JM, Schumacher J, Jacobson ER.** 1995. Immunoperoxidase detection of ophidian paramyxovirus in snake lung using a polyclonal antibody. J. Vet. Diagn. Invest. **7:**72–77. http://dx.doi.org/10.1177/104063879500700111.
32. **Franke J, Essbauer S, Ahne W, Blahak S.** 2001. Identification and molecular characterization of 18 paramyxoviruses isolated from snakes. Virus Res. **80:**67–74. http://dx.doi.org/10.1016/S0168-1702(01)00353-7.